CILAMCE 2017
Florianópolis - Santa Catarina - Brazil

DETERMINATION OF MATERIAL CONSTANTS FOR A LINEARLY ELASTIC PERIDYNAMIC MATERIAL

Adair R. Aguiar

Alan B. Seitenfuss

aguiarar@sc.usp.br

alanbour@usp.br

Dept. of Structural Engineering, São Carlos School of Engineering, University of São Paulo

Av. Trabalhador São-carlense, 400, 13566-590 - São Carlos, São Paulo, Brazil.

Abstract. *Peridynamics is a nonlocal theory that extends the classical continuum theory by considering collective motion of all the material within a* δ*-neighborhood of any point of a peridynamic body. It considers the interaction of material points due to forces acting at a finite distance smaller than* δ*, which is called the peridynamic horizon. A relation between interaction force and relative displacement between particles is proposed in Aguiar and Fosdick (2014) for an isotropic linear elastic peridynamic material. The relation is derived from a free energy function that depends quadratically on measures of strain that are analogous to the measures of strain of the classical linear theory. The energy function contains four peridynamic material constants; three of which were determined in previous work by using both convergence results of the peridynamic theory to the classical linear elasticity theory and a correspondence argument between the proposed free energy function and the strain energy density function from the classical linear elasticity theory. In previous presentation we have also shown an expression for the fourth material constant, which was obtained from the correspondence argument by evaluating both the peridynamic free energy and the strain energy at a specific point of a beam bent by terminal couples. In this work we show that this expression is valid regardless of the point chosen inside the beam. Also, we have considered two additional experiments to verify the validity of the expressions obtained for all the peridynamic constants. This work is of interest in all areas of continuum mechanics, such as in fracture mechanics, where surfaces of discontinuities exist, or, may appear as a result of deformation.*

Keywords: *Nonlocal Theory, Peridynamics, Free Energy Function, Elasticity, Fracture Mechanics*

1 INTRODUCTION

Peridynamics is a nonlocal theory that extents the classical continuum theory by considering collective motion of all the material within a δ-neighborhood of any point of a peridynamic body. It considers the interaction of material points due to forces acting at a finite distance smaller than δ, which is called the peridynamic horizon and corresponds to a length scale that is treated as a material property related to the microstructure of the body.

These forces are related to relative displacements, and the balance of linear momentum is formulated as an integral equation that remains valid across a surface of discontinuity, or, a continuum in which discontinuities may appear as a result of deformation. Away from these places, where the deformation is smooth, peridynamics yields the same governing equations of the classical continuum theory in the limit of vanishing distances between material points.

A relation between interaction force and relative displacement between particles is presented by Aguiar and Fosdick (2014) for an isotropic linear elastic peridynamic material. The relation is derived from a free energy function that depends quadratically on measures of strain that are analogous to the measures of strain of the classical linear theory. The free energy function contains four peridynamic material constants. Using homogeneous deformations and expressions presented by Silling (2010) that relate the elasticity tensor from the classical linear theory to its counterpart in peridynamics, called the modulus state, Aguiar and Fosdick (2014) derive two relations between the two Lamé constants and three peridynamic constants, leaving, therefore, one constant in these two relations as arbitrary.

To determine the arbitrary constant, Aguiar (2016) introduces a decomposition of the relative displacement in terms of radial and non-radial components. If the radial component is zero, the free energy function reduces to an integral expression that multiplies the arbitrary constant. This result is then used in a correspondence argument between the free energy function evaluated at any material point and a weighted average of the strain energy function of classical linear theory in a δ-neighborhood of this point, yielding a general expression for the determination of the arbitrary constant. To generate the zero radial component, Aguiar and Fosdick (2014) considers the torsion of a circular shaft in equilibrium without body force. The resulting expression together with the previous two expressions yield the three peridynamic constants referred to above. The procedure described above to determine the third arbitrary constant is used by Seitenfuss, Aguiar and Pereira (2016) to determine the fourth peridynamic material constant. For this, the authors consider the experiment of a cylindrical beam bent by terminal couples and evaluate both the peridynamic free energy function and the weighted average of the strain energy function at the origin of the coordinate system, which is located at the center of one end of the beam.

This work consists of verifying the validity of the expressions obtained for the peridynamic material constants. In order to do this, we consider again the experiment of a cylindrical beam bent by terminal couples, but do not restrict the previous evaluations to the origin of the coordinate system. We also consider other experiments in mechanics, such as bending of a beam by terminal load and anti-plane shear of a circular cylinder. Analytical and numerical results indicate that the expressions for the four peridynamic constants are independent of the experiment chosen.

In summary, in Section 2 we present preliminary results concerning the kinematics of small deformations, which is used in the presentation of the free energy function of an isotropic simple elastic material containing four peridynamic coefficients. We then review the procedure to obtain three of these coefficients in Section 2.3 and the fourth one in Section 2.4. Recall from above that, for the fourth coefficient, we calculate both the peridynamic free energy function and the weighted average of the classical strain energy density at the center of an end of a beam bent by terminal couples. In Section 3.1 we show that the expression for the fourth constant does not depend on the particular choice of a material point inside this beam. In Section 3.2 we consider the experiment of an elastic beam bent by terminal load and use it to verify the validity of the expressions found for the four peridynamic constants. For this, we evaluate numerically the free energy function and the classical strain energy density function for this experiment and use these calculations to verify that the correspondence argument mentioned above is approximately satisfied for given values of mechanical and geometrical properties and at different material points inside the beam. A similar verification is conducted in Section 3.3, where we consider the experiment of a circular cylinder subjected to anti-plane shear. In Section 4 we present concluding remarks.

2 PRELIMINARY RESULTS

Preliminary results of this work are summarized below for completeness. The results presented in Section 2.1-2.3 are detailed in both Aguiar and Fosdick (2014) and Aguiar (2016), while the results of Section 2.4 are detailed in Seitenfuss, Aguiar and Pereira (2016).

2.1 Kinematics of small deformation

Let $\mathcal{B} \in \mathbb{E}^3$ be the undistorted reference configuration of a body and $\mathbf{x} \in \mathcal{B}$ be a material point of $\mathcal{B}$, as illustrated in Fig. 1. Let also $N_\delta(\mathbf{x}_0) \subset \mathcal{B}$ be a neighborhood of any point $\mathbf{x}_0 \in \mathcal{B}$. Here, $N_\delta(\mathbf{x}_0)$ is a sphere of radius δ centered at $\mathbf{x}_0$. For $\mathbf{x}_0 \in N_\delta(\mathbf{x}_0)$, the vector $\boldsymbol{\xi} := \mathbf{x} - \mathbf{x}_0$ is called a bond of $\mathbf{x}$ to $\mathbf{x}_0$ and $\mathcal{H}_\delta(\mathbf{x}_0)$ is the collection of all bonds to $\mathbf{x}_0$.

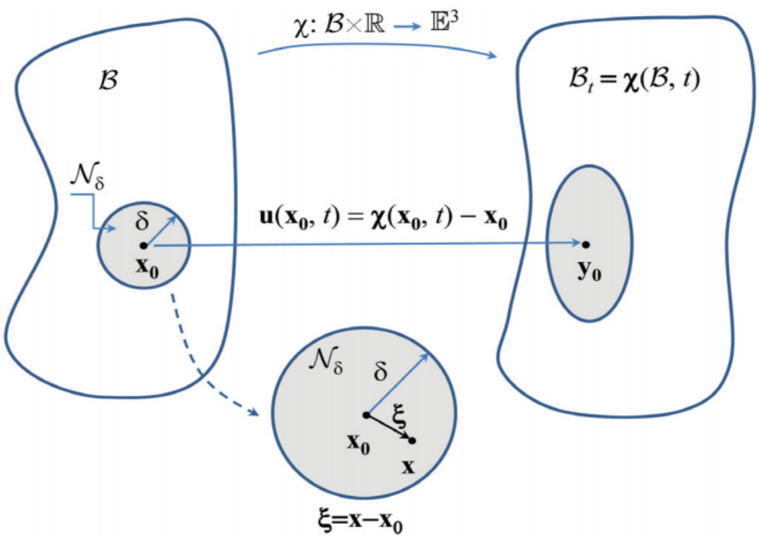

Figure 1: Reference and deformed configurations of a body. Source: Aguiar and Fosdick (2014).

A peridynamic state at $(\mathbf{x}_0, t)$ of order m is a function $\underline{\mathbf{A}}(\mathbf{x}_0, t)\langle\cdot\rangle : \mathcal{H}_\delta(\mathbf{x}_0) \to \mathcal{L}_m$, where $\mathcal{L}_m$ is the set of all tensors of order m. Thus, the image of a bond $\xi \in \mathcal{H}_\delta(\mathbf{x}_0)$ for the state $\underline{\mathbf{A}}(\mathbf{x}_0, t)\langle\cdot\rangle$ is the tensor of order m, $\underline{\mathbf{A}}(\mathbf{x}_0, t)\langle\boldsymbol{\xi}\rangle$. We denote by $\mathcal{A}_m$ the set of all states at $(\mathbf{x}_0, t)$ of order m. Similarly, we introduce the definition of a double state at $(\mathbf{x}_0, t)$ of order p, $\underline{\underline{\mathbf{D}}}(\mathbf{x}_0, t)\langle\cdot,\cdot\rangle : \mathcal{H}_\delta(\mathbf{x}_0) \times \mathcal{H}_\delta(\mathbf{x}_0) \to \mathcal{L}_p$. The dependency between two states $\underline{\mathbf{A}}(\mathbf{x}_0, t)\langle\cdot\rangle : \mathcal{H}_\delta(\mathbf{x}_0) \to \mathcal{L}_m$ and $\underline{\mathbf{u}}(\mathbf{x}_0, t)\langle\cdot\rangle : \mathcal{H}_\delta(\mathbf{x}_0) \to \mathcal{L}_p$ is denoted by $\underline{\mathbf{A}}(\mathbf{x}_0, t)\langle\boldsymbol{\xi}\rangle = \widehat{\underline{\mathbf{A}}}(\mathbf{x}_0, t)[\underline{\mathbf{u}}]\langle\boldsymbol{\xi}\rangle$. For notational convenience, we shall not exhibit the dependence on the time variable t and, when the meaning is clear, may also omit the dependence on the particle $\mathbf{x}_0$.

The difference deformation state $\underline{\boldsymbol{\chi}} \in \mathcal{A}_1$ at $\mathbf{x}_0 \in \mathcal{B}$ is defined through

$$\underline{\boldsymbol{\chi}}\langle\boldsymbol{\xi}\rangle := (\boldsymbol{\chi}(\mathbf{x}) - \boldsymbol{\chi}(\mathbf{x}_0))\,|_{\mathbf{x}=\mathbf{x}_0+\boldsymbol{\xi}}\,,$$

where $\boldsymbol{\chi}(\mathbf{x})$ is the motion of particle $\mathbf{x}$ at time t. A similar definition holds for the difference displacement state $\underline{\mathbf{u}} \in \mathcal{A}_1$ at $\mathbf{x}_0 \in \mathcal{B}$, which is given by

$$\underline{\mathbf{u}}\langle\boldsymbol{\xi}\rangle := (\mathbf{u}(\mathbf{x}) - \mathbf{u}(\mathbf{x}_0))\,|_{\mathbf{x}=\mathbf{x}_0+\boldsymbol{\xi}}\,,$$

where $\mathbf{u}(\mathbf{x})$ is the displacement of particle $\mathbf{x}$ at time t. With $\underline{\mathbf{x}} \in \mathcal{A}_1$ being the reference position vector state at $\mathbf{x}_0 \in \mathcal{B}$, so that $\underline{\mathbf{x}}\langle\boldsymbol{\xi}\rangle \equiv \boldsymbol{\xi} = \mathbf{x} - \mathbf{x}_0$, we may write $\underline{\boldsymbol{\xi}} = \underline{\mathbf{u}} + \underline{\mathbf{x}}$. The difference deformation and displacement quotient states at $\mathbf{x}_0 \in \mathcal{B}$ are then defined by

$$\underline{\mathbf{f}} := \frac{\underline{\boldsymbol{\chi}}}{|\underline{\mathbf{x}}|} = \underline{\mathbf{h}} + \underline{\mathbf{e}}, \qquad \underline{\mathbf{h}} := \frac{\underline{\mathbf{u}}}{|\underline{\mathbf{x}}|}, \tag{1}$$

respectively, where $\underline{\mathbf{e}} := \underline{\mathbf{x}}/\,|\underline{\mathbf{x}}|$ and $|\underline{\mathbf{A}}|$ is the magnitude state of $\underline{\mathbf{A}}$, defined through $|\underline{\mathbf{A}}|\,\langle\boldsymbol{\xi}\rangle := \sqrt{\underline{\mathbf{A}}\langle\boldsymbol{\xi}\rangle \cdot \underline{\mathbf{A}}\langle\boldsymbol{\xi}\rangle}$, with " $\cdot$ " being the scalar product in $\mathbb{E}^3$.

The difference displacement quotient state at $\mathbf{x}_0 \in \mathcal{B}$, defined in Eq. (1), can be decomposed as

$$\underline{\mathbf{h}}\langle\boldsymbol{\xi}\rangle = \underline{\varphi}\langle\boldsymbol{\xi}\rangle\underline{\mathbf{e}}\langle\boldsymbol{\xi}\rangle + \underline{\mathbf{h}}_d\langle\boldsymbol{\xi}\rangle, \tag{2}$$

where $\underline{\varphi}$ is a scalar state that yields the radial component of $\underline{\mathbf{h}}\langle\boldsymbol{\xi}\rangle$ and $\underline{\mathbf{h}}_d$ is a vector state that satisfies $\underline{\mathbf{h}}_d\langle\boldsymbol{\xi}\rangle \cdot \underline{\mathbf{e}}\langle\boldsymbol{\xi}\rangle = 0$.

2.2 The peridynamic material

The peridynamic equation of motion is given by (Aguiar and Fosdick, 2014)

$$\rho(\mathbf{x}_0)\ddot{\mathbf{u}}(\mathbf{x}_0) = \int_{N_\delta} \{\underline{\mathbf{L}}(\mathbf{x}_0)\langle\mathbf{x} - \mathbf{x}_0\rangle - \underline{\mathbf{L}}(\mathbf{x})\langle\mathbf{x}_0 - \mathbf{x}\rangle\} dv_x + \mathbf{b}(\mathbf{x}_0), \tag{3}$$

where ρ is the mass density, $\mathbf{u}$ is the displacement field, $\mathbf{b}$ is a prescribed body force density, and $\underline{\mathbf{L}}(\mathbf{x}_0)\langle\cdot\rangle$ is the force vector state evaluated on bonds at $\mathbf{x}_0$. Equation (3) is the counterpart in peridynamics of the differential equation of balance of linear momentum from the classical theory.

For a simple elastic material near its natural state, Aguiar and Fosdick (2014) show that

$$\underline{\mathbf{L}}(\mathbf{x}_0) \equiv \widehat{\underline{\mathbf{L}}}_{\mathbf{x}_0}[\underline{\mathbf{h}}] = \frac{\delta_{\underline{\mathbf{h}}}\widehat{W}_{\mathbf{x}_0}[\underline{\mathbf{h}}]}{|\underline{\mathbf{x}}|}, \tag{4}$$

where $\delta_{\underline{\mathbf{h}}}$ is the Fréchet derivative with respect to $\underline{\mathbf{h}}$ and $\widehat{W}_{\mathbf{x}_0}[\underline{\mathbf{h}}]$ is a free energy function.

Aguiar (2016) uses the decomposition in Eq. (2) to present an alternative form for the quadratic free energy function of a simple elastic material proposed by Aguiar and Fosdick (2014). It is given by

$$\widehat{W}_{\mathbf{x}_0}[\underline{\mathbf{h}}] = \widehat{W}_{\mathbf{x}_0}[\underline{\varphi}\,\underline{\mathbf{e}}] + \widehat{W}_{\mathbf{x}_0}[\underline{\mathbf{h}}_d] + \frac{\widehat{\alpha}_{13}}{2}\int_{N_\delta} \underline{\mathbf{h}}_d\langle\boldsymbol{\xi}\rangle \cdot \int_{N_\delta} \frac{\omega(|\boldsymbol{\xi}|,|\boldsymbol{\eta}|)}{\sin\alpha}(\underline{\varphi}\langle\boldsymbol{\xi}\rangle + \underline{\varphi}\langle\boldsymbol{\eta}\rangle)\underline{\mathbf{e}}\langle\boldsymbol{\eta}\rangle dv_\eta dv_\xi, \quad (5)$$

where $\omega(\cdot,\cdot)$ is a given symmetric weighting function,

$$\widehat{W}_{\mathbf{x}_0}[\underline{\varphi}\,\underline{\mathbf{e}}] = \frac{1}{2}\int_{N_\delta} \underline{\varphi}\langle\boldsymbol{\xi}\rangle \cdot \int_{N_\delta} \omega(|\boldsymbol{\xi}|,|\boldsymbol{\eta}|)[\widehat{\alpha}_{11}\underline{\varphi}\langle\boldsymbol{\xi}\rangle + 2\alpha_{12}\underline{\varphi}\langle\boldsymbol{\eta}\rangle] dv_\eta dv_\xi, \quad (6)$$

$$\widehat{W}_{\mathbf{x}_0}[\underline{\mathbf{h}}_d] = \frac{\alpha_{33}}{4}\int_{N_\delta} \underline{\mathbf{h}}_d\langle\boldsymbol{\xi}\rangle \cdot \int_{N_\delta} \frac{\omega(|\boldsymbol{\xi}|,|\boldsymbol{\eta}|)}{(\sin\alpha)^2}[\underline{\mathbf{e}}\langle\boldsymbol{\eta}\rangle \cdot \underline{\mathbf{h}}_d\langle\boldsymbol{\xi}\rangle + \underline{\mathbf{e}}\langle\boldsymbol{\xi}\rangle \cdot \underline{\mathbf{h}}_d\langle\boldsymbol{\eta}\rangle]\underline{\mathbf{e}}\langle\boldsymbol{\eta}\rangle dv_\eta dv_\xi, \quad (7)$$

and $\widehat{\alpha}_{11},\ \alpha_{12},\ \widehat{\alpha}_{13}$, and α_{33} are elastic peridynamic constants.

Substituting Eq. (5) thru Eq. (7) into Eq. (4), we get

$$\begin{aligned}\underline{\underline{\widehat{\mathbf{L}}_{\mathbf{x}_0}}}[\underline{\mathbf{h}}]\langle\boldsymbol{\xi}\rangle = &\int_{N_\delta} \frac{\omega(|\boldsymbol{\xi}|,|\boldsymbol{\eta}|)}{|\boldsymbol{\xi}|}\Big\{\widehat{\alpha}_{11}\underline{\varphi}\langle\boldsymbol{\xi}\rangle\underline{\mathbf{e}}\langle\boldsymbol{\xi}\rangle + 2\alpha_{12}\underline{\varphi}\langle\boldsymbol{\eta}\rangle\underline{\mathbf{e}}\langle\boldsymbol{\xi}\rangle \\ &+ \frac{\alpha_{33}}{2\sin\alpha}\left(\underline{\mathbf{e}}\langle\boldsymbol{\eta}\rangle \cdot \underline{\mathbf{h}}_d\langle\boldsymbol{\xi}\rangle + \underline{\mathbf{e}}\langle\boldsymbol{\xi}\rangle \cdot \underline{\mathbf{h}}_d\langle\boldsymbol{\eta}\rangle\right)\underline{\underline{\mathbf{e}}}\langle\boldsymbol{\xi},\boldsymbol{\eta}\rangle \\ &+ \frac{\widehat{\alpha}_{13}}{2}\left[(\underline{\varphi}\langle\boldsymbol{\xi}\rangle + \underline{\varphi}\langle\boldsymbol{\eta}\rangle)\underline{\underline{\mathbf{e}}}\langle\boldsymbol{\xi}\boldsymbol{\eta}\rangle + \frac{1}{\sin\alpha}(\underline{\mathbf{e}}\langle\boldsymbol{\eta}\rangle \cdot \underline{\mathbf{h}}_d\langle\boldsymbol{\xi}\rangle + \underline{\mathbf{e}}\langle\boldsymbol{\xi}\rangle \cdot \underline{\mathbf{h}}_d\langle\boldsymbol{\eta}\rangle)\underline{\mathbf{e}}\langle\boldsymbol{\xi}\rangle\right]\Big\}dv_\eta. \quad (8)\end{aligned}$$

2.3 Determination of three peridynamic constants

Using convergence results obtained by Silling and Lehoucq (2008), Aguiar and Fosdick (2014) show that, for a homogeneous deformation corresponding to an infinitesimal displacement gradient $\mathbf{H}_0$,

$$\frac{1}{2}\mathbf{H}_0 \cdot (\mathbb{C}_{\mathbf{x}_0}\mathbf{H}_0) = \widehat{W}_{\mathbf{x}_0}[\mathbf{H}_0\underline{\mathbf{e}}], \quad (9)$$

where $\mathbb{C}_{\mathbf{x}_0}$ is the elasticity tensor of the classical linear theory and $\widehat{W}_{\mathbf{x}_0}[\underline{\mathbf{h}}]$ is given by Eq. (5) together with both Eq. (6) and Eq. (7). They further show that the left-hand side of the relation in Eq. (9) reduces to the strain energy function of an isotropic classical linear elastic material, which is given by

$$\widehat{W}^L_{\mathbf{x}_0}[\mathbf{E}] = \frac{1}{2}[\lambda(tr\mathbf{E})^2 + 2\mu\mathbf{E}\cdot\mathbf{E}], \quad (10)$$

where λ and μ are the Lamé constants and $\mathbf{E} := (\mathbf{H}_0 + \mathbf{H}_0^T)/2$ is the infinitesimal strain tensor. Using the resulting relation between $\widehat{W}^L_{\mathbf{x}_0}[\underline{\mathbf{h}}]$, given by Eq. (10), and $\widehat{W}_{\mathbf{x}_0}[\underline{\mathbf{h}}]$, given by Eq. (5) thru Eq. (7), the authors obtain two relations between the peridynamic material constants $\widehat{\alpha}_{11},\ \alpha_{12},\ \alpha_{33}$ and classical elasticity constants. These relations are given by

$$2\widehat{\alpha}_{11} + \alpha_{33} = \frac{15E}{16(1+\nu)\omega_\delta}, \quad \widehat{\alpha}_{11} + 2\alpha_{12} = \frac{3E}{16(1-2\nu)\omega_\delta}, \quad (11)$$

where $\nu = \lambda/[2\,(\lambda+\mu)]$ is the Poisson's ratio, $E = \mu\,(3\,\lambda+2\,\mu)/(\lambda+\mu)$ the Young's modulus, and $\omega_\delta \equiv \pi^2 \int_0^\delta \int_0^\delta \omega(\check{\rho},\hat{\rho})\check{\rho}^2\hat{\rho}^2 d\hat{\rho}d\check{\rho}$.

To obtain a third relation, Aguiar (2016) introduces a correspondence argument according to which the free energy function of the peridynamic material at $\mathbf{x}_0$ near the natural state is equal to the weighted average of the strain energy density function from classical elasticity theory in a δ-neighborhood of $\mathbf{x}_0$. Assuming that the multiplicative decomposition

$$\omega(|\boldsymbol{\xi}|,|\boldsymbol{\eta}|) = \widetilde{\omega}(|\boldsymbol{\xi}|)\widetilde{\omega}(|\boldsymbol{\eta}|)|\boldsymbol{\xi}|^2|\boldsymbol{\eta}|^2 \tag{12}$$

holds, where $\widetilde{\omega} : \mathbb{R} \to \mathbb{R}$ is a known weighting function, the correspondence argument yields

$$\widehat{W}_{\mathbf{x}_0}[\underline{\mathbf{h}}] = \overline{W}^L_{\mathbf{x}_0}[\underline{\mathbf{h}}] := \frac{1}{m}\int_{N_\delta} \widetilde{\omega}(|\boldsymbol{\xi}|)\,|\boldsymbol{\xi}|^2\,\widehat{W}^L_{\mathbf{x}_0}[\widehat{\mathbf{E}}[\underline{\mathbf{h}}]]dv_\xi, \tag{13}$$

where $\widehat{\mathbf{E}}[\underline{\mathbf{h}}]$ is the infinitesimal strain tensor obtained from the vector state $\underline{\mathbf{h}}$ and

$$m := \int_{N_\delta} \widetilde{\omega}(|\boldsymbol{\xi}|)|\boldsymbol{\xi}|^2 dv_{\boldsymbol{\xi}}. \tag{14}$$

Observe from Eq. (13) with $\widehat{\mathbf{E}}[\underline{\mathbf{h}}]$ constant that $\widehat{W}_{\mathbf{x}_0}[\underline{\mathbf{h}}] = \widehat{W}^L_{\mathbf{x}_0}[\widehat{\mathbf{E}}[\underline{\mathbf{h}}]]$. Therefore, Eq. (9) with both its left-hand side replaced by Eq. (10) and $\omega(\cdot,\cdot)$ given by Eq. (12) is a particular case of Eq. (13).

Considering the infinitesimal deformation of a homogeneous, isotropic, and linearly elastic circular shaft under uniform torsion and using Eq. (13), Aguiar (2016) obtains the relation

$$\alpha_{33} = \frac{20\mu}{m^2}. \tag{15}$$

Replacing Eq. (15) and the expressions $\mu = E/(2(1+\nu))$ and $\kappa = E/(3(1-2\nu))$ into Eq. (11), the other two contants can also be determined, being given by

$$\widehat{\alpha}_{11} = \frac{5\mu}{m^2}, \quad \alpha_{12} = \frac{1}{2m^2}(9\kappa - 5\mu)\,. \tag{16}$$

2.4 Determination of fourth peridynamic constant, $\hat{\alpha}_{13}$

In this section and in Section 3 we use a fixed orthonormal basis $\{\mathbf{e}_1,\,\mathbf{e}_2,\,\mathbf{e}_3\}$ associated to the Cartesian coordinates $(\xi_1,\,\xi_2,\,\xi_3)$ with origin at the centroid of the left end of a prismatic bar, which is aligned with the ξ_3-direction. The bar is homogeneous, isotropic and linearly elastic. To perform numerical integrations, we use the software MATHEMATICA 9 © with a global adaptive strategy.

We now review the procedure employed by Seitenfuss, Aguiar and Pereira (2016) in the determination of the fourth peridynamic constant, $\hat{\alpha}_{13}$. This constant represents nonlocal effects of the peridynamic material and can not be determined from the approach leading to the expressions in Eq. (11). To determine $\hat{\alpha}_{13}$, we consider a simple experiment in mechanics that provides a deformation field for which both radial and non-radial components of $\underline{\mathbf{h}}$ in (2) do not vanish.

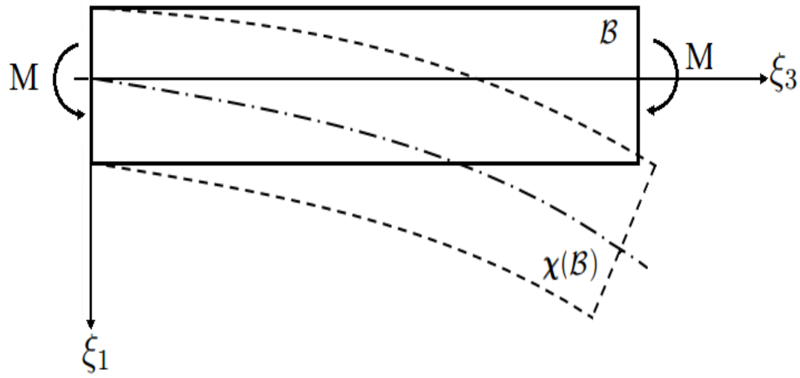

Figure 2: Beam bent by terminal couples.

The experiment consists of a beam bent by terminal couples in equilibrium with no body force, as illustrated in Fig. 2. The lateral surface of the beam is free of traction. In classical linear elasticity, the corresponding displacement field is given by (Sokolnikoff, 1956)

$$\mathbf{u}(\xi_1, \xi_2, \xi_3) = \frac{M}{2EI}[({\xi_3}^2 + \nu{\xi_1}^2 - \nu{\xi_2}^2)\mathbf{e}_1 + 2\nu\xi_1\xi_2\mathbf{e}_2 - 2\xi_1\xi_3\mathbf{e}_3], \tag{17}$$

where $M > 0$ is the magnitude of the bending moment, I is the moment of inertia with respect to the ξ_2-direction, and we recall from Eq. (11) that ν is the Poisson's ratio and E is the Young's modulus. The non-zero components of the corresponding infinitesimal strain tensor $\mathbf{E}$ are given by

$$\epsilon_{11} = \epsilon_{22} = \frac{M}{EI}\nu\xi_1, \quad \epsilon_{33} = -\frac{M}{EI}\xi_1. \tag{18}$$

To apply the correspondence argument presented in Section 2.3 we first consider that $\mathbf{x}_0$ in Eq. (13) is at the origin of the coordinate system and recall from Section 2.1 that N_δ is a sphere with center at this point. We then use Eq. (10) together with $\widehat{\mathbf{E}}[\underline{\mathbf{h}}] \equiv \mathbf{E}(\xi_1, \xi_2, \xi_3)$ and the strain components given by Eq. (18) to obtain $(M^2/2EI^2)\xi_1^2$ in the integrand on the right hand side of Eq. (13). Using the coordinate transformation

$$\xi_1 = \rho\ cos\theta\ sin\phi, \quad \xi_2 = \rho\ sin\theta\ sin\phi, \quad \xi_3 = \rho\ cos\phi, \tag{19}$$

and taking the limits of integration

$$\rho \in (0, \delta), \quad \phi \in (0, \pi), \quad \theta \in (0, 2\pi), \tag{20}$$

we obtain

$$\overline{W}^L_{\mathbf{x}_0}[\underline{\mathbf{h}}] = \frac{M^2 m_6}{6EI^2 m_4}, \tag{21}$$

where m_4 and m_6 are given by the general expression

$$m_n := 4\pi \int_0^\delta \widetilde{\omega}(\rho)\rho^n d\rho, \quad n = 1, 2, ... \tag{22}$$

Observe from both Eq. (14) and Eq. (22) that $m = m_4$.

To determine the expressions of $\underline{\mathbf{h}}_d\langle\boldsymbol{\xi}\rangle$ and $\underline{\varphi}\langle\boldsymbol{\xi}\rangle$ in Eq. (2) for this experiment, first, we use the definition in Eq. (1.b) together with

$$\underline{\mathbf{u}}\langle\boldsymbol{\xi}\rangle := (\mathbf{u}(\mathbf{x}) - \mathbf{u}(\mathbf{x}_0))\,|_{\mathbf{x}=\mathbf{x}_0+\boldsymbol{\xi}}, \tag{23}$$

and recall that $\mathbf{x}_0$ is at the origin to obtain $\underline{\mathbf{h}}\langle\boldsymbol{\xi}\rangle = \mathbf{u}(\rho,\phi,\theta)/\rho$ where $\mathbf{u}(\rho,\phi,\theta)$ can be obtained from Eq. (17) by using the coordinate transformation in Eq. (19) together with the change of basis

$$\begin{aligned}
&\mathbf{e}_1 = cos\theta\, sin\phi\, \mathbf{e}_\rho + cos\theta\, cos\phi\, \mathbf{e}_\phi - sin\theta\, \mathbf{e}_\theta,\\
&\mathbf{e}_2 = sin\theta\, sin\phi\, \mathbf{e}_\rho + sin\theta\, cos\phi\, \mathbf{e}_\phi + cos\theta\, \mathbf{e}_\theta, \quad \mathbf{e}_3 = cos\phi\, \mathbf{e}_\rho + sin\phi\, \mathbf{e}_\phi.
\end{aligned} \tag{24}$$

Using the additive decomposition in Eq. (2), we then get the radial and non-radial components of $\underline{\mathbf{h}}\langle\boldsymbol{\xi}\rangle$, which are given by, respectively,

$$\underline{\varphi}\langle\boldsymbol{\xi}\rangle = \frac{M\rho}{2EI} cos\theta\; sin\phi(\nu^2\phi - cos^2\phi), \tag{25}$$

$$\underline{\mathbf{h}}_d\langle\boldsymbol{\xi}\rangle = \frac{M\rho}{4EI}\{-cos\phi\; cos\theta[-3-\nu+(1+\nu)cos(2\phi)]\mathbf{e}_\phi + 2sin\theta(\nu^2\phi - cos^2\phi)\mathbf{e}_\theta\}.$$

Next, we use the multiplicative decomposition of $\omega(|\boldsymbol{\xi}|,|\boldsymbol{\eta}|)$, given in Eq. (12), Eq. (25) and the limits of integration in Eq. (20) into Eq. (5), Eq. (6) and Eq. (7) to get

$$\begin{aligned}
\widehat{W}_{\mathbf{x}_0}[\underline{\mathbf{h}}] =& \hat{\alpha}_{11}\,\frac{mm_6}{840}\frac{M^2}{(EI)^2}(24\nu^2 - 8\nu + 3) + \alpha_{33}\,\frac{mm_6}{6720}\frac{M^2}{(EI)^2}(64\nu^2 + 16\nu + 92)\\
&+ \hat{\alpha}_{13}\,\frac{\pi {m_5}^2}{3360}\frac{M^2}{(EI)^2}(-11\nu^2 + 20\nu - 4),
\end{aligned} \tag{26}$$

where both $m \equiv m_4$ and m_6 are given in Eq. (22). The terms in Eq. (26) that multiply α_{33} and $\hat{\alpha}_{13}$ were calculated by numerical integration.

Substituting the expresions in Eq. (26) together with Eq. (21) into Eq. (13), we can solve the resulting equation for $\hat{\alpha}_{13}$, yielding

$$\hat{\alpha}_{13} = \frac{140}{\pi}\frac{m_6\,\mu}{m\,m_5^2}\frac{8\nu^2 - 8\nu - 1}{11\nu^2 - 20\nu + 4}, \tag{27}$$

where we have used the expressions of $\hat{\alpha}_{11}$, α_{12}, and α_{33} given by Eq. (15) and Eq. (16).

3 VALIDATION OF EXPRESSIONS FOR MATERIAL CONSTANTS

So far, we have obtained the expressions in both Eq. (15) and Eq. (16) by considering homogeneous deformations in Aguiar and Fosdick (2014) and the uniform torsion of a circular shaft in Aguiar (2016). We have also obtained Eq. (27) by considering a beam bent by terminal couples in Seitenfuss, Aguiar and Pereira (2016). In that work, $\mathbf{x}_0$ is at the origin of the left end of the beam. To verify the validity of these expressions, in Section 3.1 we consider that $\mathbf{x}_0$ is an arbitrary point of the beam and substitute the expressions of the peridynamic constants in the governing equations of the terminal couples problem. We then repeat this procedure in Section 3.2 for the case of a beam bent by terminal load and in Section 3.3 for the case of a circular shaft subjected to anti-plane shear.

3.1 Pure bending experiment

The expression in Eq. (27) was obtained by evaluating the free energy function at the origin of the coordinate system, that is, at the center of the left end of the beam. Below, we calculate both the peridynamic free energy function using the expressions of the peridynamic constants, given by Eq. (15), Eq. (16), and Eq. (27), and the classical strain energy density at an arbitrary material point of the beam. We then verify if the correspondence argument in Eq. (13) is satisfied.

To obtain the infinitesimal strain tensor $\mathbf{E}$ evaluated at $\mathbf{x}_0 = (x_0,\, y_0,\, z_0)$, we substitute

$$\xi_1 = \widehat{\xi}_1 + x_0, \quad \xi_2 = \widehat{\xi}_2 + y_0, \quad \xi_3 = \widehat{\xi}_3 + z_0 \tag{28}$$

into the expressions in Eq. (18), where $(\widehat{\xi}_1, \widehat{\xi}_2, \widehat{\xi}_3)$ are the components of the relative position vector $\boldsymbol{\xi}$. Using the coordinate transformations in Eq. (19) for $(\widehat{\xi}_1,\, \widehat{\xi}_2,\, \widehat{\xi}_3)$ and taking the limits of integration in Eq. (20), we obtain

$$\overline{W}^{L}_{\mathbf{x}_0}[\underline{\mathbf{h}}] = \frac{M^2}{EI^2}\left(\frac{{x_0}^2}{2} + \frac{m_6}{6m}\right), \tag{29}$$

where both $m = m_4$ and m_6 are given in Eq. (22). Observe from Eq. (29) that only the first term within the parentheses depends upon the position $\mathbf{x}_0$ and that the remaining term yields Eq. (21).

Next, we use Eq. (1.b) together with Eq. (23), where $\mathbf{u}(\mathbf{x})$ is given by Eq. (17), to obtain

$$\begin{aligned}\underline{\mathbf{h}}\langle\boldsymbol{\xi}\rangle =& \frac{M}{2EI\,|\boldsymbol{\xi}|}\Big(\Big\{ \widehat{\xi}_3\,(2z_0 + \widehat{\xi}_3) + \nu\left[\widehat{\xi}_1^2 + 2z_0\,\widehat{\xi}_1 - \widehat{\xi}_2\,(2y_0 + \widehat{\xi}_2)\right]\Big\}\,\mathbf{e}_1 \\ &+ 2\nu\left[y_0\,\widehat{\xi}_1 + (x_0 + \widehat{\xi}_1)\widehat{\xi}_2\right]\mathbf{e}_2 - 2\left[z_0\widehat{\xi}_1 + (x_0 + \widehat{\xi}_1)\widehat{\xi}_3\right]\mathbf{e}_3\Big).\end{aligned} \tag{30}$$

Similarly as before, we use Eq. (2) to decompose $\underline{\mathbf{h}}\langle\boldsymbol{\xi}\rangle$, given by Eq. (30), into radial and non-radial components, which are given by

$$\underline{\varphi}\langle\boldsymbol{\xi}\rangle = \underline{\mathbf{h}}\langle\boldsymbol{\xi}\rangle \cdot \underline{\mathbf{e}}\langle\boldsymbol{\xi}\rangle \;\text{ and }\; \underline{\mathbf{h}}_d\langle\boldsymbol{\xi}\rangle = \underline{\mathbf{h}}\langle\boldsymbol{\xi}\rangle - \underline{\varphi}\langle\boldsymbol{\xi}\rangle\underline{\mathbf{e}}\langle\boldsymbol{\xi}\rangle, \tag{31}$$

respectively. Using the coordinate transformation in Eq. (19) to write these expressions in spherical coordinates, substituting the resulting expressions in the integrands of Eq. (5) thru Eq. (7), and using the limits of integration in Eq. (20), we obtain

$$\begin{aligned}\widehat{W}_{\mathbf{x}_0}[\underline{\varphi}\,\underline{\mathbf{e}}] =& \frac{\hat{\alpha}_{11}}{2}\left(\frac{M}{EI}\right)^2\left[m^2\frac{1}{15}(3 - 4\nu + 8\nu^2){x_0}^2 + m_6\,m\,\frac{3 - 8\nu + 24\nu^2}{420}\right] \\ &+ \alpha_{12}\left(\frac{M}{EI}\right)^2\frac{m^2}{9}(1 - 2\nu)^2{x_0}^2.\end{aligned} \tag{32}$$

Observe from Eq. (32) that the second term inside the square brackets yields the expression which multiplies $\hat{\alpha}_{11}$ in Eq. (26) and that the remaining terms are position dependent and proportional to ${x_0}^2$.

We use numerical integration to calculate the integrals that multiply $\hat{\alpha}_{13}$ in Eq. (5) and α_{33} in Eq. (7). We divide the integrands into ten parts that correspond to multiplications by the ten monomials $1,\ x_0,\ y_0,\ z_0,\ {x_0}^2,\ {y_0}^2,\ {z_0}^2,\ x_0\, y_0,\ x_0\, z_0$, and $y_0\, z_0$. Then, we divide again each one of these parts into terms that multiply $1,\ \nu$, and ν^2, and, finally, integrate numerically each one of the resulting parts.

Concerning the integrals that multiply $\hat{\alpha}_{13}$ above, the ones that multiply terms in the set $\{x_0,\ y_0,\ z_0,\ {x_0}^2,\ {y_0}^2,\ {z_0}^2,\ x_0\, y_0,\ x_0\, z_0,\ y_0\, z_0\}$ are nearly zero when compare to the remaining three integrals that multiply 1. These integrals yield

$$\left[\frac{\pi {m_5}^2}{3360}\frac{M^2}{(EI)^2}(-11\nu^2+20\nu-4)\right], \tag{33}$$

which is the same expression that multiplies $\hat{\alpha}_{13}$ in Eq. (26).

Concerning the integrals that multiply α_{33} above, in addition to the position independent terms, also the terms that multiply ${x_0}^2$ do not vanish. A procedure similar to the one presented above for the calculation of the terms that multiply $\hat{\alpha}_{13}$ yields

$$\widehat{W}_{\mathbf{x}_0}[\underline{\mathbf{h}}_d] = \alpha_{33}\frac{M^2}{(EI)^2}\left[m^2\,(1+\nu)^2\frac{{x_0}^2}{45} + \frac{m\, m_6}{64}\frac{(64\nu^2+16\nu+92)}{105}\right]. \tag{34}$$

Replacing Eq. (32), Eq. (33), and Eq. (34) into Eq. (5) and using the expressions in Eq. (15), Eq. (16), and Eq. (27) for the peridynamic constants, we finally obtain

$$\widehat{W}_{\mathbf{x}_0}[\underline{\mathbf{h}}] = \frac{M^2}{EI^2}\left(\frac{{x_0}^2}{2} + \frac{m_6}{6m}\right), \tag{35}$$

which is equal to $\widehat{W}^L_{\mathbf{x}_0}[\underline{\mathbf{h}}]$ in Eq. (29), satisfying, therefore, the correspondence argument in the form of Eq. (13).

3.2 Bending by terminal load experiment

Consider a homogeneous, isotropic, and linearly elastic cylindrical beam of length l in equilibrium with no body force and subjected to a terminal load of magnitude P, which acts downwards on the right end of the beam, as illustrated in Fig. 3. The left end of the beam is fixed and, as in Section 2.4, its lateral surface is free of traction. Recalling from Section 2.4 that the origin of the Cartesian coordinates $(\xi_1,\ \xi_2,\ \xi_3)$ is at the centroid of the left end of the beam, the corresponding displacement field is given by (Sokolnikoff, 1956)

$$\begin{aligned}\mathbf{u}(\xi_1,\xi_2,\xi_3) =& \frac{P}{EI}\Bigg\{\frac{1}{2}\Big[\nu(l-\xi_3)({\xi_1}^2-{\xi_2}^2) - \frac{1}{3}{\xi_3}^3 + l\,{\xi_3}^2\Big]\mathbf{e}_1 + \nu\,\xi_1\,\xi_2(l-\xi_3)\,\mathbf{e}_2 \\ &- \Big[\Phi(\xi_1,\xi_2) + \xi_1{\xi_2}^2 + (l\,\xi_3 - \frac{1}{2}{\xi_3}^2)\xi_1\Big]\mathbf{e}_3\Bigg\},\end{aligned} \tag{36}$$

where $\Phi(\xi_1,\xi_2)$ is the classical Saint-Venant flexure function, which is harmonic and, therefore, satisfies

$$\frac{\partial^2\Phi}{\partial {\xi_1}^2} + \frac{\partial^2\Phi}{\partial {\xi_2}^2} = 0 \quad \text{in } \mathcal{B}. \tag{37}$$

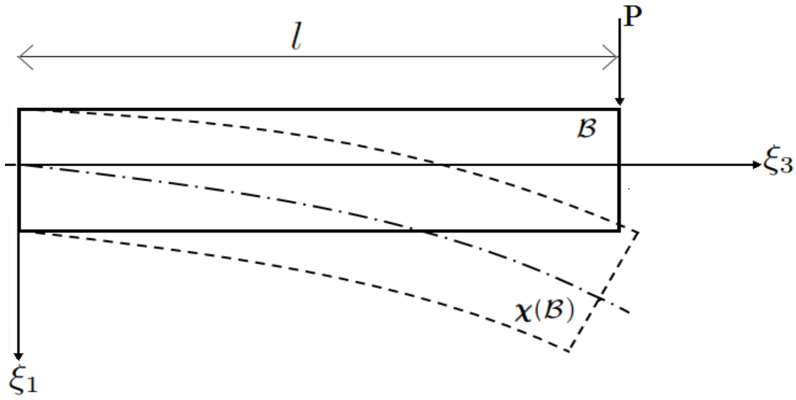

Figure 3: Beam subjected to terminal load.

For zero external force on the lateral surface Ω of the beam, Φ must satisfy

$$\nabla\Phi\cdot\mathbf{n} = -\left[\frac{1}{2}\nu{\xi_1}^2 + (1-\frac{1}{2}\nu){\xi_2}^2\right] cos(\xi_1,\mathbf{n}) - (2+\nu)\xi_1\,\xi_2\, cos(\xi_2,\mathbf{n}) \qquad \text{on} \quad \Omega, \quad (38)$$

where $\nabla(\cdot)$ is the gradient operator in $\mathbb{R}^3$ and $\mathbf{n}$ denotes the exterior unit normal vector to the boundary Ω.

If Ω is the lateral surface of a circular cylinder, the solution of the system of differential equations in both Eq. (37) and Eq. (38) is given by

$$\Phi(\xi_1,\xi_2) = \frac{1}{4}({\xi_1}^3 - 3\,\xi_1\,{\xi_2}^2) - \frac{a^2}{4}\,\xi_1(3+2\,\nu), \quad (39)$$

where a is the radius of the cross section of the cylinder.

Replacing Eq. (39) into Eq. (36) and using the definition $\mathbf{E} := (\text{grad}\,\mathbf{u} + \text{grad}\,\mathbf{u}^T)/2$, we find that the matrix representation of the infinitesimal strain tensor $\mathbf{E}$ in the basis $\{\mathbf{e}_1,\, \mathbf{e}_2,\, \mathbf{e}_3\}$ is given by

$$[\mathbf{E}] = \frac{P}{EI}\begin{bmatrix} \nu\,\xi_1(l-\xi_3) & 0 & \frac{[(a^2-{\xi_1}^2)(3+2\nu)+(2\nu-1){\xi_2}^2]}{8} \\ 0 & \nu\,\xi_1(l-\xi_3) & -\frac{(1+2\nu)\xi_1\,\xi_2}{4} \\ \frac{[(a^2-{\xi_1}^2)(3+2\nu)+(2\nu-1){\xi_2}^2]}{8} & -\frac{(1+2\nu)\xi_1\,\xi_2}{4} & \xi_1(l-\xi_3) \end{bmatrix}. \quad (40)$$

We substitute the coordinates in Eq. (28) into Eq. (40) and evaluate $\widehat{W}^L_{\mathbf{x}_0}[\widehat{\mathbf{E}}[\underline{\mathbf{h}}]]$ using Eq. (10). We then use the resulting expression for $\widehat{W}^L_{\mathbf{x}_0}[\widehat{\mathbf{E}}[\underline{\mathbf{h}}]]$ and the transformations in Eq. (19) for $(\widehat{\xi}_1,\, \widehat{\xi}_2,\, \widehat{\xi}_3)$ together with the limits of integration in Eq. (20) to evaluate $\overline{W}^L_{\mathbf{x}_0}[\underline{\mathbf{h}}]$, which is defined in Eq. (13). The resulting expression is rather long and will not be presented here. Below we do present, however, numerical values for this expression.

To evaluate the integrals of the peridynamic free energy function, given by Eq. (5) thru Eq. (7), we use Eq. (1.b), Eq. (23), and Eq. (36) to obtain $\underline{\mathbf{h}}\langle\boldsymbol{\xi}\rangle$ and then Eq. (31) to obtain $\underline{\varphi}\langle\boldsymbol{\xi}\rangle$ and $\underline{\mathbf{h}}_d\langle\boldsymbol{\xi}\rangle$. Substituting $\underline{\varphi}\langle\boldsymbol{\xi}\rangle$ and $\underline{\mathbf{h}}_d\langle\boldsymbol{\xi}\rangle$ into Eq. (5) thru Eq. (7), we obtain integrals multiplying

$\hat{\alpha}_{13}$ and α_{33} that do not seem to be possible to evaluate analytically. For this reason, in this subsection we introduce numerical values for both the material and the geometrical properties of the beam. The values of the material properties are

$$\nu = 1/4,\ \delta = 0.1\,a, \tag{41}$$

and the geometrical properties are

$$l = 5\,a,\ I = \pi\,a^4/4,\ \ a = 1\,\text{unit of length.} \tag{42}$$

Since the parameters P and E appear only in the ratio P^2/E on both sides of the equality in Eq. (13), we take $P = 1$ N and $E = 1$ Pa. Also, we consider that

$$\widetilde{\omega}(|\boldsymbol{\xi}|) = \frac{1}{|\boldsymbol{\xi}|^2}. \tag{43}$$

Moreover, the peridynamic free energy function and the strain energy density are calculated for a set of arbitrary points inside the domain, as explained below.

Using the values given in Eq. (41), the expression in Eq. (43), and the expressions in Eq. (15), Eq. (16), and Eq. (27), the numerical values for the peridynamic constants are

$$\hat{\alpha}_{11} \approx 113986\,\frac{\text{N}}{\text{m}^8}, \quad \alpha_{12} \approx 113986\,\frac{\text{N}}{\text{m}^8}, \quad \alpha_{33} \approx 455945\,\frac{\text{N}}{\text{m}^8}, \quad \hat{\alpha}_{13} \approx 8669212\,\frac{\text{N}}{\text{m}^8}. \tag{44}$$

In the general case, these values must be multiplied by E to obtain the peridynamic constants of a linearly elastic material having $\nu = 1/4$. Observe from Eq. (44) that the approximate values of $\hat{\alpha}_{11}$ and α_{12} are equal to each other, a fact that could be anticipated from the last paragraph of Section 2.3 by considering $\nu = 1/4$ in the expressions of E and κ and then substituting the resulting expressions in Eq. (16).

In Table 1 we show the values of the numerical integrations at nine different points. The parameters A_{11}, A_{12}, A_{33}, and A_{13} are integrals that multiply $\hat{\alpha}_{11}$, α_{12}, α_{33}, and $\hat{\alpha}_{13}$, respectively, and are defined by

$$\begin{aligned}
A_{11} &:= \int_{N_\delta} \widetilde{\omega}(|\boldsymbol{\xi}|)\,|\boldsymbol{\xi}|^2\,\underline{\varphi}\langle\boldsymbol{\xi}\rangle^2 \int_{N_\delta} \widetilde{\omega}(|\boldsymbol{\eta}|)\,|\boldsymbol{\eta}|^2\,dv_\eta dv_\xi,\\
A_{12} &:= \int_{N_\delta} \widetilde{\omega}(|\boldsymbol{\xi}|)\,|\boldsymbol{\xi}|^2\,\underline{\varphi}\langle\boldsymbol{\xi}\rangle \int_{N_\delta} \widetilde{\omega}(|\boldsymbol{\eta}|)\,|\boldsymbol{\eta}|^2\,\underline{\varphi}\langle\boldsymbol{\eta}\rangle dv_\eta dv_\xi,\\
A_{33} &:= \int_{N_\delta} \widetilde{\omega}(|\boldsymbol{\xi}|)\,|\boldsymbol{\xi}|^2\,\underline{\mathbf{h}}_d\langle\boldsymbol{\xi}\rangle \cdot \int_{N_\delta} \frac{\widetilde{\omega}(|\boldsymbol{\eta}|)\,|\boldsymbol{\eta}|^2}{(sin\alpha)^2}(\underline{\mathbf{e}}\langle\boldsymbol{\eta}\rangle \cdot \underline{\mathbf{h}}_d\langle\boldsymbol{\xi}\rangle + \underline{\mathbf{e}}\langle\boldsymbol{\xi}\rangle \cdot \underline{\mathbf{h}}_d\langle\boldsymbol{\eta}\rangle)\underline{\mathbf{e}}\langle\boldsymbol{\eta}\rangle dv_\eta dv_\xi,\\
A_{13} &:= \int_{N_\delta} \widetilde{\omega}(|\boldsymbol{\xi}|)\,|\boldsymbol{\xi}|^2\,\underline{\mathbf{h}}_d\langle\boldsymbol{\xi}\rangle \cdot \int_{N_\delta} \frac{\widetilde{\omega}(|\boldsymbol{\eta}|)\,|\boldsymbol{\eta}|^2}{sin\alpha}(\underline{\varphi}\langle\boldsymbol{\xi}\rangle + \underline{\varphi}\langle\boldsymbol{\eta}\rangle)\underline{\mathbf{e}}\langle\boldsymbol{\eta}\rangle dv_\eta dv_\xi.
\end{aligned} \tag{45}$$

Table 1: Results of numerical integrations for the beam bent by terminal load.

(x_0, y_0, z_0)	A_{11}	A_{12}	A_{33}	A_{13}
(0, 0, 0)	$1.47583 \cdot 10^{-6}$	0	$1.70017 \cdot 10^{-6}$	$2.36814 \cdot 10^{-9}$
(0.2, 0, 0)	$6.10305 \cdot 10^{-6}$	$7.90119 \cdot 10^{-7}$	$5.5376 \cdot 10^{-6}$	$2.34618 \cdot 10^{-9}$
(0.4, 0, 0)	$2.00126 \cdot 10^{-5}$	$3.16048 \cdot 10^{-6}$	$1.70792 \cdot 10^{-5}$	$2.87896 \cdot 10^{-9}$
(0.6, 0, 0)	$4.32881 \cdot 10^{-5}$	$7.11117 \cdot 10^{-6}$	$3.64024 \cdot 10^{-5}$	$2.61717 \cdot 10^{-9}$
(0.8, 0, 0)	$7.6069 \cdot 10^{-5}$	$1.26419 \cdot 10^{-5}$	$6.36532 \cdot 10^{-5}$	$2.86705 \cdot 10^{-9}$
(0, 0.4, 0)	$1.41031 \cdot 10^{-6}$	0	$1.63497 \cdot 10^{-6}$	$2.3393 \cdot 10^{-9}$
(0, 0, 2)	$1.45957 \cdot 10^{-6}$	0	$2.1033 \cdot 10^{-6}$	$7.11753 \cdot 10^{-10}$
(0.4, 0.4, 0)	$1.99851 \cdot 10^{-5}$	$3.16048 \cdot 10^{-6}$	$1.70503 \cdot 10^{-5}$	$2.45249 \cdot 10^{-9}$
(0.4, 0.4, 0.4)	$1.70685 \cdot 10^{-5}$	$2.67503 \cdot 10^{-6}$	$2.3794 \cdot 10^{-5}$	$2.0836 \cdot 10^{-9}$

In the second thru the fifth columns of Table 2 we show the result of the multiplication of the peridynamic constants in Eq. (46) by the parameters defined in Eq. (47) with the corresponding values given in Table 1. In the last two columns of Table 2 we show the values of the peridynamic free energy function and the weighted average of the strain energy density. Notice that the values at the sixth column, corresponding to $\widehat{W}_{\mathbf{x}_0}[\underline{\mathbf{h}}]$, are the sum of the four columns to its left hand side. Comparison between the last two columns shows that the correspondence argument in Eq. (13) is approximately satisfied for the experiment of a beam bent by terminal load at the nine selected points and using the material and geometrical parameters given by Eq. (41) and Eq. (42), respectively. The maximum percentage error between the two columns, defined by

$$(\widehat{W}_{\mathbf{x}_0}[\underline{\mathbf{h}}] - \overline{W}^L_{\mathbf{x}_0}[\underline{\mathbf{h}}]) * 100/\overline{W}^L_{\mathbf{x}_0}[\underline{\mathbf{h}}]\,, \tag{46}$$

is 0.18%, which is small if we take into account that the integrals were evaluated numerically.

Table 2: The free energy function and the strain energy density for the beam bent by terminal load.

(x_0, y_0, z_0)	$A_{11} \cdot \hat{\alpha}_{11}/2$	$A_{12} \cdot \alpha_{12}$	$A_{33} \cdot \alpha_{33}/4$	$A_{13} \cdot \hat{\alpha}_{13}/2$	$\widehat{W}_{\mathbf{x}_0}[\underline{\mathbf{h}}]$	$\overline{W}^L_{\mathbf{x}_0}[\underline{\mathbf{h}}]$
(0, 0, 0)	0.084112	0	0.193796	0.010265	0.2881728	0.287635
(0.2, 0, 0)	0.3478324	0.090063	0.631211	0.01017	1.0792755	1.078947
(0.4, 0, 0)	1.1405797	0.36025	1.946794	0.012479	3.4601029	3.457646
(0.6, 0, 0)	2.4671303	0.810578	4.149386	0.011344	7.4384384	7.438045
(0.8, 0, 0)	4.33542	1.441003	7.255569	0.012427	13.04442	13.04394
(0, 0.4, 0)	0.0803783	0	0.186365	0.01014	0.2768827	0.276508
(0, 0, 2)	0.0831855	0	0.239748	0.003085	0.3260186	0.326543
(0.4, 0.4, 0)	1.1390122	0.360251	1.943502	0.010631	3.4533964	3.45301
(0.4, 0.4, 0.4)	0.9727806	0.304915	2.712194	0.009032	3.9989214	3.999269

In Fig. 4 we present curves obtained from the numerical values of $\widehat{W}_{\mathbf{x}_0}[\underline{\mathbf{h}}]$ and $\overline{W}^L_{\mathbf{x}_0}[\underline{\mathbf{h}}]$ shown in the first four lines of Table 2, which correspond to evaluations of $\widehat{W}_{\mathbf{x}_0}[\underline{\mathbf{h}}]$ and $\overline{W}^L_{\mathbf{x}_0}[\underline{\mathbf{h}}]$ along the x_0-axis. We can see from the graph that there is no visible difference between the two curves. Performing multiple regression with the software NLREG for the data of $\widehat{W}_{\mathbf{x}_0}[\underline{\mathbf{h}}]$

and x_0 from Table 2, we get the best regression for a biquadratic function, which has the form $\widehat{W}_{\mathbf{x}_0}[\underline{\mathbf{h}}] = 0.24020592\,{x_0}^4 + 19.7774191\,{x_0}^2 + 0.288290755$, and the coefficient of determination $R^2 = 0.999999975$. Also, in view of Eq. (28), Eq. (10), and Eq. (13), we can see from Eq. (40) that $\overline{W}^L_{\mathbf{x}_0}[\underline{\mathbf{h}}]$ is a quartic polynomial of x_0 having the form $\alpha_1\,{x_0}^4 + \alpha_2\,{x_0}^3 + \alpha_3\,{x_0}^2 + \alpha_4\,x_0 + \alpha_5$ for $y_0 = z_0 = 0$. From the result of the regression analysis and the observation of some additional results of integration not shown here, we conclude that the coefficients of x_0 and ${x_0}^3$ vanish and that $\overline{W}^L_{\mathbf{x}_0}[\underline{\mathbf{h}}]$ depend biquadratically on x_0. In fact, using the numerical values presented in this section, we obtain $\overline{W}^L_{\mathbf{x}_0}[\underline{\mathbf{h}}] = 0.248237\,{x_0}^4 + 19.7729\,{x_0}^2 + 0.287636$, which is very similar to the expression obtained for $\widehat{W}_{\mathbf{x}_0}[\underline{\mathbf{h}}]$ shown above.

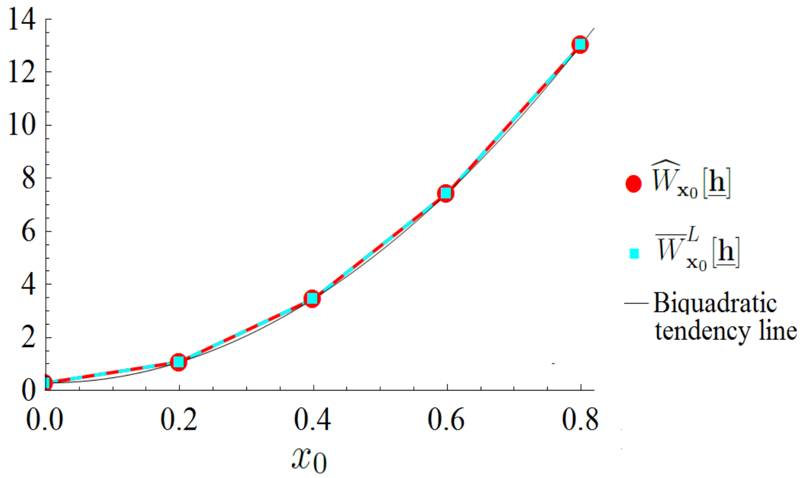

Figure 4: Numerical values of $\widehat{W}_{\mathbf{x}_0}[\mathbf{h}]$ and $\overline{W}^L_{\mathbf{x}_0}[\mathbf{h}]$ versus x_0 for $y_0 = z_0 = 0$.

3.3 Anti-plane shear experiment

We now consider the anti-plane shear deformation of a homogeneous, isotropic, and linearly elastic circular hollow cylinder in equilibrium with no body force. The inner and the outer surfaces of the cylinder are submitted to constant displacements of magnitudes β and α, respectively, which are paralell to the generators of the cylinder, as illustrated in Fig. 5. The ends of the cylinder are free of traction.

In classical linear elasticity, the displacement field of the anti-plane shear problem stated above has the form

$$\mathbf{u} = u_3(\xi_1, \xi_2)\,\mathbf{e}_3, \tag{47}$$

where $u_3 : \mathcal{B} \to \mathbb{R}$ must be harmonic in $\mathcal{B}$ to satisfy equilibrium and is radially symmetric with respect to the center of the hollow cylinder. It is not difficult to show that

$$u_3(\xi_1,\, \xi_2) = \frac{\alpha - \beta}{ln\,(r_1/r_2)}\, ln\,\sqrt{{\xi_1}^2 + {\xi_2}^2} + \frac{ln\,({r_1}^{\beta}/{r_2}^{\alpha})}{ln\,(r_1/r_2)}, \tag{48}$$

where r_1 and r_2 are, respectivelly, the inner and the outer radii of the cylinder.

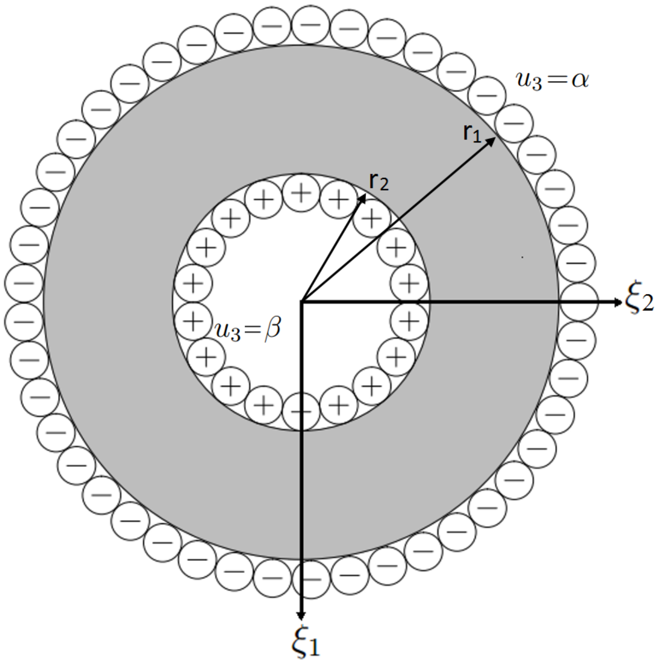

Figure 5: Shaft subjected to anti-plane shear.

The non-zero components of the infinitesimal strain tensor $\mathbf{E}$ in the basis $\{\mathbf{e}_1,\, \mathbf{e}_2,\, \mathbf{e}_3\}$ are given by

$$\epsilon_{i2} = \frac{(\beta-\alpha)\,\xi_i}{2\,({\xi_1}^2+{\xi_2}^2)\,ln\,(r_1/r_2)}, \quad i=1,\,2. \tag{49}$$

This tensor is used in Eq. (10) to obtain the strain energy density of the hollow cylinder at a point $\mathbf{x}_0 \in \mathcal{B}$, which is given by

$$\overline{W}^L_{\mathbf{x}_0}[\mathbf{E}] = \mu \left[\frac{\alpha-\beta}{ln\,(r_1/r_2)}\right]^2 \frac{1}{\xi_1^2+\xi_2^2}.$$

Substituting this expression in the definition of Eq. (13) and using Eq. (43), we obtain

$$\overline{W}^L_{\mathbf{x}_0}[\underline{\mathbf{h}}] = \frac{\mu}{m}\int_{N_\delta} \frac{1}{\xi_1^2+\xi_2^2} dv_\xi \left[\frac{\alpha-\beta}{ln\,(r_1/r_2)}\right]^2 .$$

Now, recall from Section 3.2 that the integrals multiplying the peridynamic constants $\widehat{\alpha}_{11}$, α_{12}, $\widehat{\alpha}_{13}$, and α_{33} in Eq. (5) thru Eq. (7) are given by the parameters A_{11}, A_{12}, A_{33}, and A_{13}, respectivelly, which are defined in Eq. (45). Again, we consider that $\widetilde{\omega}(|\boldsymbol{\xi}|)$ is given by Eq. (43). To obtain the expressions of $\underline{\varphi}\langle\boldsymbol{\xi}\rangle$ and $\underline{\mathbf{h}}_d\langle\boldsymbol{\xi}\rangle$ in Eq. (45), we use Eq. (48) and the procedure explained in Section 3.2. We then find that

$$\begin{aligned} \underline{\varphi}\langle\boldsymbol{\xi}\rangle &= (\beta-\alpha)\,\xi_3\,\frac{ln\,(\xi_1^2+\xi_2^2) - 2\,ln\sqrt{(\xi_1+x_0)^2+(\xi_2+y_0)^2}}{2\,(\xi_1^2+\xi_2^2+\xi_3^2)\,ln\,(r_1/r_2)}\,, \\ \underline{\mathbf{h}}_d\langle\boldsymbol{\xi}\rangle &= -\underline{\varphi}\langle\boldsymbol{\xi}\rangle\,\left[\xi_1\,\xi_3\,\mathbf{e}_1 + \xi_2\,\xi_3\,\mathbf{e}_2 + (\xi_1^2+\xi_2^2)\,\mathbf{e}_3\right]. \end{aligned} \tag{50}$$

To evaluate numerically the parameters in Eq. (45) and the peridynamic constants in Eq. (15) and Eq. (16), we take

$$\nu = 1/4,\ E = 1\ \text{Pa},\ \delta = r_1/16 \tag{51}$$

for the material properties and

$$r_2 = r_1/2,\ r_1 = 8 \text{ units of length} \tag{52}$$

for the geometrical properties. It then follows from Eq. (15) and Eq. (16) that

$$\hat{\alpha}_{11} \approx 7.29513\,\frac{\text{N}}{\text{m}^8},\quad \alpha_{12} \approx 7.29513\,\frac{\text{N}}{\text{m}^8},\quad \alpha_{33} \approx 29.1805\,\frac{\text{N}}{\text{m}^8},\quad \hat{\alpha}_{13} \approx 554.83\,\frac{\text{N}}{\text{m}^8}. \tag{53}$$

The factor $\mu\,(\beta-\alpha)^2/[ln\,(r_1/r_2)^2]$ appears on both sides of Eq. (13) and is omitted below. The last term of Eq. (48), which contains α and β, represents a rigid body translation and does not contribute to both energy terms in Eq. (13). As in the case of Eq. (44), the approximate values of $\hat{\alpha}_{11}$ and α_{12} in Eq. (53) are equal to each other.

Because the problem is symmetric, we can expect that the numerical results depend only on the radial position of a point and not on its angular position. In fact, results obtained for points on different radial lines and at the same distance from the origin do not differ from each other. For this reason, we only show the results for the points on the ξ_2-axis.

In Table 3 we present results of numerical integrations at seven different points along the ξ_2-axis, which lie 4.5, 5, 5.5, 6, 6.5, 7 and 7.5 units of length far from the origin. In this table the values of the peridynamic constants $\widehat{\alpha}_{11}$, α_{12}, $\widehat{\alpha}_{13}$, and α_{33} are given in Eq. (53) and the parameters A_{11}, A_{12}, A_{33} and A_{13} are the integrals defined in (45). The last two columns of Table 3 contain values of the free energy function and the weighted average of the strain energy density. Comparing these two columns, we see that, also for the anti-plane shear problem, the correspondence argument in the form of Eq. (13) is approximately satisfied at the selected points for the material and geometrical properties given by Eq. (51) and Eq. (52), respectively. Using Eq. (46), the maximum percentage error between the values of the two columns is 0.017%, which is very small if we take into account that the integrals were evaluated numerically..

Table 3: The free energy function and the strain energy density for the anti-plane shear problem.

(x_0, y_0)	$A_{11}\cdot\hat{\alpha}_{11}/2$	$A_{12}\cdot\alpha_{12}$	$A_{33}\cdot\alpha_{33}/4$	$A_{13}\cdot\hat{\alpha}_{13}/2$	$\widehat{W}_{\mathbf{x}_0}[\underline{\mathbf{h}}]$	$\overline{W}^L_{\mathbf{x}_0}[\underline{\mathbf{h}}]$
(0, 7.5)	0,002468	0	0,004939	$6,0803\cdot 10^{-6}$	0,007413	0,007414
(0, 7)	0,002833	0	0,005671	$9,06435\cdot 10^{-6}$	0,008513	0,008513
(0, 6.5)	0,003287	0	0,006579	$1,05170\cdot 10^{-5}$	0,009877	0,009877
(0, 6)	0,003857	0	0,007723	$1,48363\cdot 10^{-5}$	0,011594	0,011595
(0, 5.5)	0,004590	0	0,009194	$2,40001\cdot 10^{-5}$	0,013808	0,013807
(0, 5)	0,005555	0	0,011129	$3,30121\cdot 10^{-5}$	0,016718	0,016718
(0, 4.5)	0,00686	0	0,013748	$4,83078\cdot 10^{-5}$	0,020655	0,020659

In Fig. 6 we have plotted the numerical values of both $\widehat{W}_{\mathbf{x}_0}[\underline{\mathbf{h}}]$ and $\overline{W}^L_{\mathbf{x}_0}[\underline{\mathbf{h}}]$ that appear in the last two columns of Table 3 against points on the ξ_2-axis that appear in the first column of that table. Again, there is very good agreement between these values. Performing power regression with the software NLREG for the data of $\widehat{W}_{\mathbf{x}_0}[\underline{\mathbf{h}}]$ and y_0 from Table 3, we obtain $\widehat{W}_{\mathbf{x}_0}[\underline{\mathbf{h}}] = 0.4221625\, y_0{}^{-2.0061641}$ and coefficient of determination $R^2 = 0.99999986$.

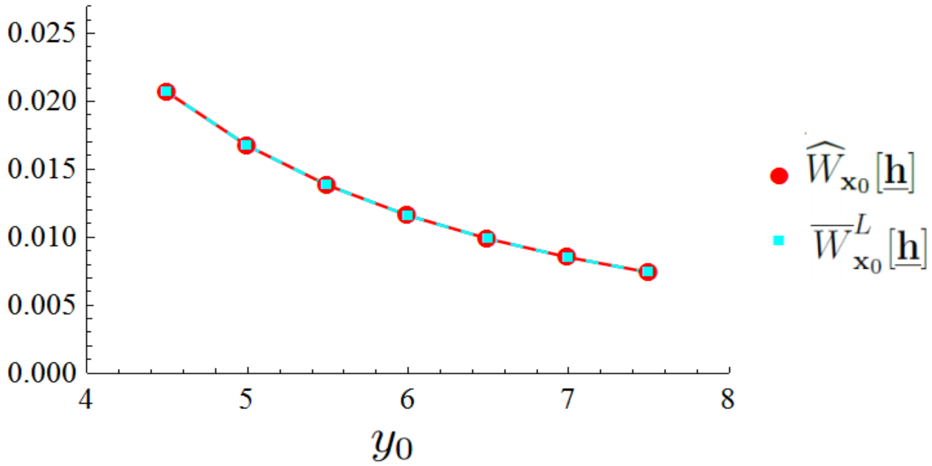

Figure 6: Numerical values of $\widehat{W}_{\mathbf{x}_0}[\mathbf{h}]$ and $\overline{W}^L_{\mathbf{x}_0}[\mathbf{h}]$ plotted for points on the ξ_2-axis.

4 CONCLUSIONS

The four peridynamic constants that appear in the free energy function defined by Eq. (5) together with Eq. (6) and Eq. (7) were previously determined using homogeneous deformations, uniform torsion of a circular shaft and bending of a beam by terminal couples. In this work, we have verified the validity of the closed form expressions for the peridynamic constants by using displacement fields from classical linear elasticity for both beam bent by terminal load and circular shaft subjected to anti-plane shear. We have considered numerical values for the material and geometrical properties and used the expressions of the peridynamic constants to numerically calculate the free energy function and the weighted average of the strain energy density at selected points in the domain.

The results shown in Table 2, Table 3, Fig. 4, and Fig. 6 indicate that the correspondence argument, given by Eq. (13) is nearly satisfied for the above experiments. We then see that the values of the peridynamic constants are not dependent on the type of experiment. This work is, therefore, an important contribution to the development of a three-dimensional state-based peridynamic theory.

ACKNOWLEDGEMENTS

The National Council for Scientific and Technological Development (CNPq), grant # 444896/2014-7, and the Coordination for the Improvement of Higher Education Personnel (CAPES) are gratefully acknowledged for providing financial support for this work.

References

Aguiar, A. R., & Fosdick, R. L., 2014. A constitutive model for a linearly elastic peridynamic body. *Mathematics and Mechanics of Solids*, vol. 19, n. 5, pp. 502–523.

Aguiar, A. R., 2016. On the Determination of a Peridynamic Constant in a Linear Constitutive Model. *Journal of Elasticity*, vol. 122, n. 1, pp. 27-39.

Seitenfuss, A. B., Aguiar, A. R., & Pereira, M., 2016. Numerical and theoretical study of the properties of a linear elastic peridynamic material. *Proceedings of the XXXV Iberian Latin-American Congress on Computational Methods in Engineering*.

Silling, S., 2010. Linearized theory of peridynamic states. *Journal of Elasticity*, vol. 99 n. 1, pp. 85–111.

Silling, S. A., & Lehoucq, R. B., 2008. Convergence of peridynamics to classical elasticity theory. *Journal of Elasticity*, vol. 93, pp. 13–37.

Sokolnikoff, I. S., 1956. *Mathematical Theory of Elasticity*. 2 ed. New York: McGraw-Hill. 476 p.